Proceedings of ICFDP7:
Seventh International Congress on Fluid Dynamics and Propulsion
December 18-20, 2001, Cairo, Egypt

ICFDP7-2001003

INFLUENCE OF VARIOUS FACTORS ON THE FLOW CHARACTERISTICS THROUGH A GAS TURBINE CASCADE

Ahmed F. Abdel Gawad
Assist. Prof., Mech. Power Eng. Dept.
Faculty of Eng., Zagazig Univ., Egypt
Member ASME, ahgawad@netscape.net

Osama E. Abdellatif
Assoc. Prof., Mech. Power Eng. Dept.
Shoubra Faculty of Eng., Zagazig Univ., Egypt
Currently: Faculty of Eng., October 6 Univ.

ABSTRACT

The influence of different factors on the flow characteristics of a gas turbine cascade was studied. These factors include blade shape, incidence angle, Reynolds number, and mainstream turbulence. Two five-blade linear cascades in a low-speed wind tunnel facility were used in the experiments. The mainstream Reynolds numbers were 202,000 and 166,000 based on the cascade inlet velocity and blade chord. The blade shapes are based on the Wortmann Fx-66 blade. Comparisons were made with the available published experimental data. The results show that there are important effects of the examined factors on the flow characteristics of the cascade. Useful practical conclusions were driven from the results.

I. INTRODUCTION

Studying the flow characteristics through turbine cascade helps greatly in understanding the effect of the different parameters on the cascade performance. Actual operating problems such as overheating and erosion of the turbine blade may be solved by comprehensive investigations of the flow characteristics through cascades. Improvements of heat transfer may be achieved by enhancing the aerodynamic characteristics of the turbine blades. Blade erosion results in changing the original (designed) blade shape. Hence, Changes in the flow characteristics are expected as the operating time increases. Thus, the modified blade shape may affect the lift coefficient on the blade. The effect of mainstream turbulence generated by the combustor and/or the upstream blade row on the aerodynamic and heat transfer performances of the blade is a crucial problem in advanced gas turbine engine design. Many investigators have studied, experimentally and theoretically, the effect of operating factors on the flow characteristics in a turbine cascade. Sharma et al. [1] investigated experimentally the development of boundary layers under the influence of velocity distributions simulating the suction sides of two-turbine airfoils. They intended to use their data to develop an improved turbulence model suitable for application on turbine airfoil design. Moore and Adhye [2] investigated experimentally the loss mechanisms and the behavior of secondary flows downstream of a large scale, linear turbine cascade. They found that the secondary flow field at each measurement plane is dominated by a single large passage vortex, which decays in strength because of the mixing occurring in the flow. More than one-third of the losses were found to occur downstream of the trailing edge. Zhang and Han [3] studied the influence of mainstream turbulence on surface heat transfer coefficients of a gas turbine blade. Their results showed that the mainstream turbulence promotes earlier and boarder boundary layer transition causes higher heat transfer coefficients on the suction surface, and significantly enhances the heat transfer coefficient on the pressure surface. Kind et al. [4] carried out measurements of pressure distributions, profile losses, and flow deviation on a planar turbine cascade in incompressible flow to asses the effects of partial roughness coverage of the blade surfaces. They found that roughness has a little effect on static pressure distribution around the blades and on deviation angle. Roughness on the suction surface can cause large increase in profile losses. Duden and Fottner [5] investigated experimentally and numerically two highly loaded linear turbine cascades with the same blade profile and stacking but with parallel end walls and divergently tapered end walls. They showed that the taper has a strong influence on the pressure distribution and causes an unexpected high rise in secondary loss. In both cascades the secondary loss coefficient rises with the reduced Reynolds and Mach numbers. Ristic and Lakshminarayana [6] measured the three-dimensional

viscous flow field development in the nozzle passage of an axial flow turbine stage using "x" hot-wire probe. They stated that the secondary flow region near the suction surface-casing corner indicated the presence of the passage vortex detached from the vane surface. Brown and Martin [7] examined the flow transition phenomena and heat transfer over the pressure surfaces of gas turbine blades. They adopted laminarization values of velocity gradient factor as a design criterion for the pressure surfaces of turbine blades. The laminarization values have significant advantages in reducing heat transfer, increasing lift, and lowering aerodynamic drag. Choi and Yoo [8] proposed an explicit fourth-order Runge-Kutta solver for the Navier-Stokes equations and an implicit approximate factorization scheme for the k-ω equations. Their results proved that the scheme is fast, stable and accurate, requiring less computer capacity than conventional fully implicit time-stepping schemes. Natalini and Sciubba [9] studied numerically a two-dimensional cascade of an internally cooled gas turbine vane. They aimed to minimize the local rates of entropy production. They concluded that the total entropy generation rate can be computed numerically from the known flowfields.

This work represents a wide experimental study of the effect of incidence angle, Reynolds number, blade shape and mainstream turbulence intensity on the flow characteristics through a gas turbine cascade. The blade profiles are based on the Wortmann Fx-66 blade section. Results include the pressure and lift coefficients. The main objective of the present study is to provide turbine designers with a database of the performance of the turbine blade under different operating conditions. Comparisons are made with the available data in the literature. Useful comments are stated.

II. NOMENCLATURE

B_1 = blade section based on Wortmann-Fx66 blade profile.

B_2 = modified blade section.

C = blade chord length.

C_L = lift coefficient.

C_p = static pressure coefficient = $\dfrac{P - P_1}{q_1}$.

C_x = blade chord length in the streamwise direction.

H = blade height.

M_L = mean loss coefficient = $\dfrac{P_{o1} - P_{o2}}{q_1}$.

P = static pressure.

P_o = mean total pressure.

q_1 = mean inlet dynamic pressure.

Re = Reynolds number based on chord length and cascade inlet velocity = $\dfrac{U_1 C}{\nu}$.

U_1 = cascade inlet velocity.

U_{max} = cascade inlet maximum velocity.

X = axial (streamwise) coordinate.

Y = blade radial (spanwise) coordinate.

α = incidence angle.

ν = kinematic viscosity of air.

Subscripts:

1, 2 = cascade up- and downstream conditions, respectively.

III. DESCRIPTION OF EXPERIMENTS

III.1 LOW-SPEED WIND TUNNEL

A low-speed open-circuit wind tunnel was used for the experimental work. A two-inlet centrifugal fan that is driven by a 4-HP AC motor drives the airflow. Inlet velocity can be adjusted to have two values of 27.5 m/s and 22.6 m/s that correspond to Reynolds numbers of 202,000 and 166,000, respectively, based on chord length and inlet velocity. The linear cascade of five blades was mounted at the exit section of the tunnel. The exit of the tunnel was equipped with side flaps that can be adjusted at the cascade outlet angle to guide the trailing edge parallel flow, see Fig. 1.

III.2 LINEAR CASCADES

The two cascades, made of good-quality model wood, had a chord of 95 mm, a span of 300 mm and a blade spacing of 60 mm. The middle blade was instrumented as a pressure tap blade. The two blade shapes are shown in Fig. 2. One of them is based on the Wortmann Fx-66 section (B1). Modifications of this section were proposed near the leading edge and the suction surface of blade (B1) to show the effect on the aerodynamic characteristics of the cascade. Hence, we get the other blade (B2).

III.3 TURBULENCE GRIDS

Fig. 3 shows a sketch of the grid that was used to increase turbulence intensity. The grid was made of round bars and located upstream of the cascade. The grid has 6mm-diameter bars and 25.4 mm bar pitch. It generates turbulence intensity of about 4 percent at the cascade inlet for Re = 166,000. The horizontal bars are placed in front of the vertical bars. A hot-wire anemometer system was used to measure inlet turbulence intensity.

III.4 PRESSURE TAP BLADE INSTRUMENTATION

Nineteen pressure taps were located in the midspan of the pressure tap instrumented blade as follows: 1 at the leading edge, 8 on the lower (pressure) surface, and 10 on the upper (suction) surface. The pressure taps were

connected to multi-tube manometer for the blade surface static pressure measurements. A Pitot probe also measured mainstream flow velocity at the inlet of the cascade.

IV. TEST CONDITIONS AND PRELIMINARY MEASUREMENTS

At the beginning, measurements were made to confirm the periodicity of velocity profiles between adjacent flow paths on either side of the middle blade (instrumented blade). Velocity profiles in the radial (spanwise) direction for two Reynolds numbers and two blade shapes at flow paths on either sides of the middle blade at inlet plane have been measured. This was done to make sure the flow in the middle part of the span is two-dimensional. The results are shown in Fig. 4. The inlet velocity profiles, for no inserted turbulence grid, are uniform between 15 and 85 percent of the span. Thus, the flow measurements are free from the effects of the top and bottom wall boundary layers. The uncertainty of the total, static pressure and velocity are 4.2, 4.7 and 5.1 percent, respectively. Error estimates were found based on the method of Ref. [10].

V. RESULTS AND DISSCUSION

V.1 EFFECT OF INCIDENCE ANGLE

The effect of incidence angle (angle of attack) on the distributions of the pressure coefficient over the upper and lower surfaces of the two blades B1 and B2 are shown in Figs. 5-8. A wide range of incidence angles, namely: α = -15^o, -10^o, -5^o, 0^o, +5^o, +10^o, and +15^o, was tested. At Re = 202,000, the increase of α to +10^o and + 15^o causes a significant decrease of the pressure on the frontal half of the upper (suction) surface of the two blades B1 and B2. At X/C_x = 0.25, Cp = -0.82 for α = +15^o while Cp = -0.21 for α = 0^o. The situation is reversed on the rear half of the upper surface of blades B1 and B2. Cp increases towards the trailing edge until it gains positive values. This behavior of Cp means higher loading in the front half of the cascade at high incidence angles (α = +10^o and +15^o). Similar behavior is noticed for Re = 166,000 up to 10% of C_x. For other incidence angles (from α = -15^o to +5^o), the pressure on the suction surface decreases gradually till it takes almost a constant value at 40% of C_x. At the lower (pressure) surface, Cp has a constant value for all angles up to 0.6 C_x where values of Cp start to decrease. Values of Cp on the lower surface, for different angles, tend to become close to each other for blade B2 especially at Re = 202,000. Changes in the pressure profiles, especially for the upper surface, are responsible for changing the lift coefficient (C_L) as will be seen later (Fig. 18). The present results are compared with the experimental results of Duden and Fottner [5] for the blade T106 at design conditions and Re = 500,000. This blade section is the closest to the present sections B1 and B2 whose data are available in the literature. Generally, the present results compare well with the published data, especially along the lower (pressure) surface. Differences on the upper (suction) surface are certainly due to the difference in the profiles of T106, B1, and B2 blades as well as difference in Reynolds number. Fig. 9 shows the effect of incidence angle on the mean loss coefficient (M_L) for different cases. The results are compared with the data of cohen et al. [11] for a reaction cascade. Evidently, the angle of incidence can vary from –15^o to +15^o without a sensible increase in M_L. The results compare very well with the data of Cohen et al. [11]. Maximum value of M_L of the published data is at α = 0^o, where the present results tend to have a minimum value at α = 0^o. However, the difference is relatively small.

V.2 EFFECT OF REYNOLDS NUMBER AND BLADE SHAPE

The effect of Reynolds number and blade shape on the pressure distributions on the upper and lower surfaces is shown in Figs. 10-16. Nearly for all incidence angles, values of Cp for Re = 202,000 are less than those for Re = 166,000 on the upper (suction) surface. This means that the loading (lift) on the cascade increases with Reynolds number, see Fig. 18. This is true for the two blades B1 and B2. As the incidence angle increases, the curves of Cp on the lower surface draw near each other and approach a value of 1.0 for the two Reynolds numbers as well as the two blades B1 and B2. Cp curves even coincide on each other starting from α = +5^o and the value of Cp is nearly 1.0 for the whole lower surface. This behavior of Cp on the lower surface contributes to the increase of loading (lift coefficient) with the increase of the incidence angle.

V.3 EFFECT OF GRID-GENERATED TURBULENCE

The effect of the grid-generated turbulence on the static pressure distribution is shown in Fig. 17. The results cover different incidence angles for blade B1 at Re = 166,000. Grid-generated turbulence has a small effect on Cp of the upper surface for most incidence angles, see Fig. 17.a. At α = +15^o, a remarkable change is noticed. Values of Cp decrease on the frontal half of the upper surface compared to the no-grid case. Also, on the rear half, Cp takes positive values. Fig. 17.b shows that for α = -5^o, -10^o, and -15^o, the grid-generated turbulence leads to higher positive values of Cp on the lower surface. This may lead to the increase of C_L. However, the general trend of the curves is maintained.

V.4 LIFT COEFFICIENT

The variation of the lift coefficient with incidence angle, for no-grid cases, is shown in Fig. 18. Generally, C_L increases with incidence angle. The rate of increase

depends on both Reynolds number and the blade shape. Some interesting observations can be driven from Fig. 18 about the behavior of C_L. For all incidence angles (from -15^o to $+15^o$), C_L of the higher Reynolds number (202,000) is higher than that of the lower Reynolds number (166,000) for both blades B1 and B2. At Re = 202,000, C_L is almost the same for the two blades B1 and B2 from $\alpha = -15^o$ to 0^o. From $\alpha = 0^o$ to $+15^o$, C_L of blade B1 is higher than that of blade B2. At $\alpha = +10^o$, C_L of B1 = 1.16 times C_L of B2. The opposite happens for Re = 166,000. From $\alpha = -15^o$ to 0^o, C_L of blade B2 is higher than that of blade B1. From $\alpha = 0^o$ to $+15^o$, lift coefficients of both blades become very close to each other.

VI. CONCLUSIONS

Measurements of pressure distributions, lift coefficients, and mean loss coefficients have been carried out on gas turbine cascades to assess the effects of incidence angle, blade shape, Reynolds number and mainstream turbulence. From the above discussions, the following comments can be driven:

1. The present results compare well to the published data.
2. The increase of Reynolds number causes higher loading on the frontal half of the blade for $\alpha = +10^o$ and $+15^o$.
3. For the present test cases, the incidence angle can vary from -15^o to = $+15^o$ without a sensible increase in mean loss coefficient (M_L).
4. The present grid-generated turbulence has a small effect on the pressure distribution on both the upper and lower surfaces of the turbine blade. This may be due to the level of turbulence examined in the present study.
5. Cascade loading (lift coefficient) depends on both Reynolds number and blade shape.
6. The loading (lift coefficient) increases with Reynolds number at all incidence angles for the two blades B1 and B2.
7. Modification of the blade shape can help in improving the lift coefficient. However, the improvement depends on Reynolds number and incidence angle.

REFERENCES

1. Sharma, O. P., Wells, R. A., Schlinker, R. H., and Bailey, D. A., 1982, "Boundary Layer Development on Turbine Airfoil Suction Surfaces," ASME Engineering for power, 104, pp. 698-705.
2. Moore, J., and Adhye, R. Y., 1985, "Secondary Flows and Losses Downstream of a Turbine Cascade," ASME Engineering for Gas Turbines and Power, 107, pp. 961-968.
3. Zhang, L., and Han, J.-C., 1994, "Influence of Mainstream Turbulence on Heat Transfer Coefficients from a Gas Turbine Blade," ASME Heat Transfer, 116, pp. 896-903.
4. Kind, R. J., Serjak, P. J., and Abbott, M. W. P., 1998, "Measurements and Prediction of the Effects of Surface Roughness on Profile Losses and Deviation in a Turbine Cascade," ASME Turbomachinery, 120, pp. 20-27.
5. Duden, A., and Fottner, L., 1997, "Influence of Taper, Reynolds Number and Mach Number on the Secondary Flow Field of a Highly Loaded Turbine Cascade," Proc. Instn. Mech. Engrs., Vol. 211, Part A, pp. 309-320.
6. Ristic, D., and Lakshminarayana, B., 1998, "Three-Dimensional Blade Boundary Layer and Endwall Flow Development in the Nozzle Passage of a Single Stage Turbine," ASME Fluids Engineering, 120, pp. 570-579.
7. Brown, A., and Martin, B. W., 1982, "Flow Transition Phenomena and Heat Transfer over the Pressure Surfaces of Gas Turbine Blades," ASME Engineering for Power, 104, pp. 360-367.
8. Choi, C. H., and Yoo, J. Y., 1997, "Cascade Flow Calculations Using the k-ω Turbulence Model with Explicit-Implicit Solver," AIAA J., Vol. 35, No. 9, pp. 1551-1552.
9. Natalini, G., and Sciubba, E., 1999, "Minimization of the Local Rates of Entropy Production in the Design of Air-Cooled Gas Turbine Blades," ASME Engineering for Gas Turbines and Power, 121, pp. 466-475.
10. Kline, S. J., and McClintock, F. A., 1953, “Describing Uncertainties in Single Sample Experiments,” Mechanical Engineering, 75.
11. Cohen, H., Rogers, G. F. C., and Saravanamuttoo, H. I. H., 1996, Gas Turbine Theory, Longman Group Limited, England.

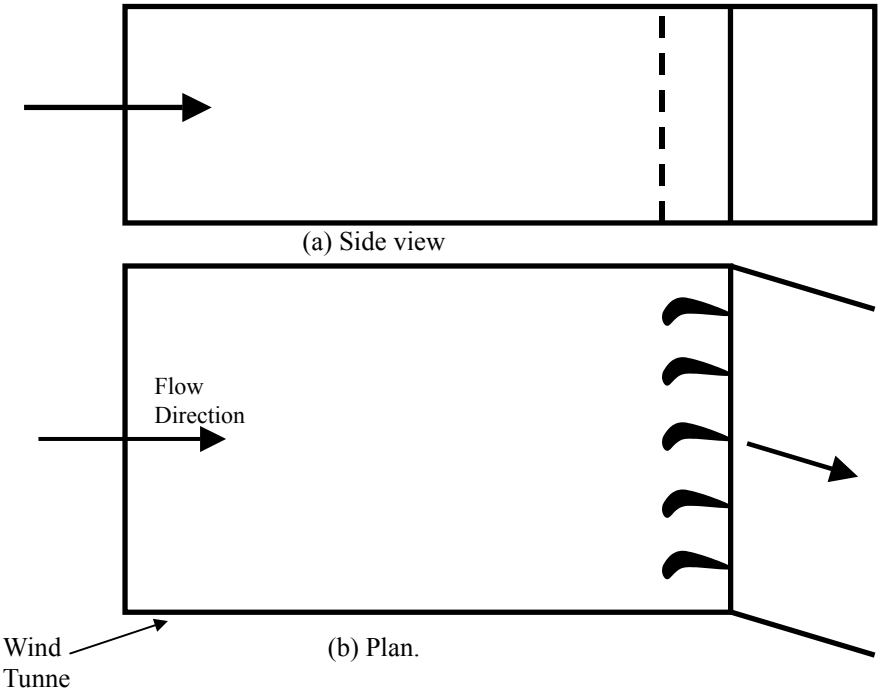

Fig. 1 Arrangement of the turbine cascade inside the wind tunnel.

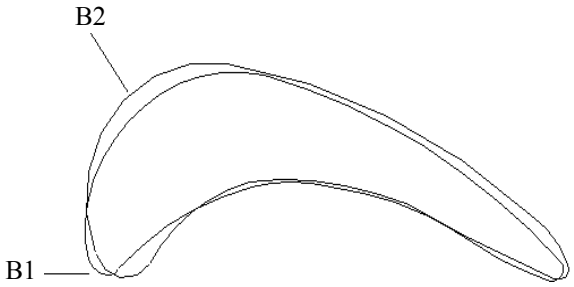

Fig. 2 Profiles of Blades (B1) and (B2).

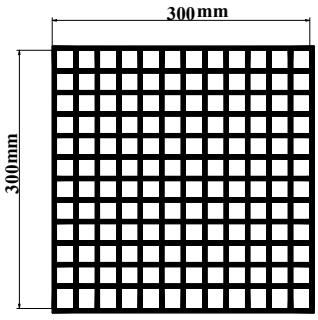

Fig. 3 Sketch of the turbulence grid.

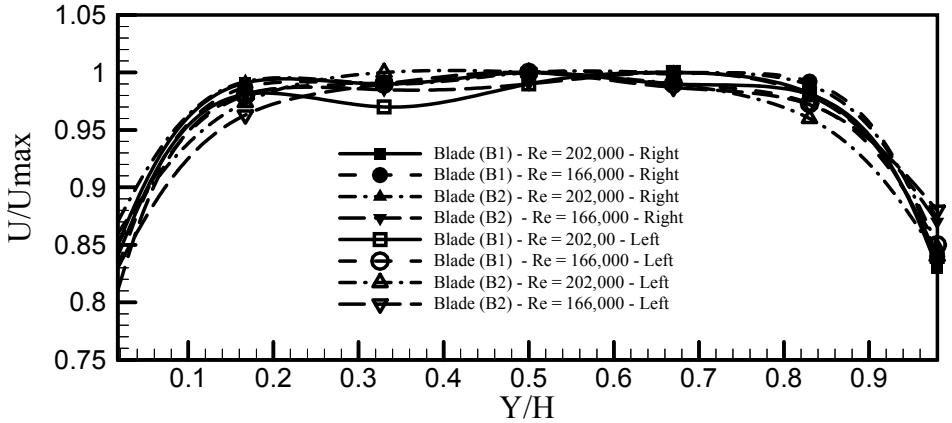

Fig. 4 Inlet velocity profiles for different cases.

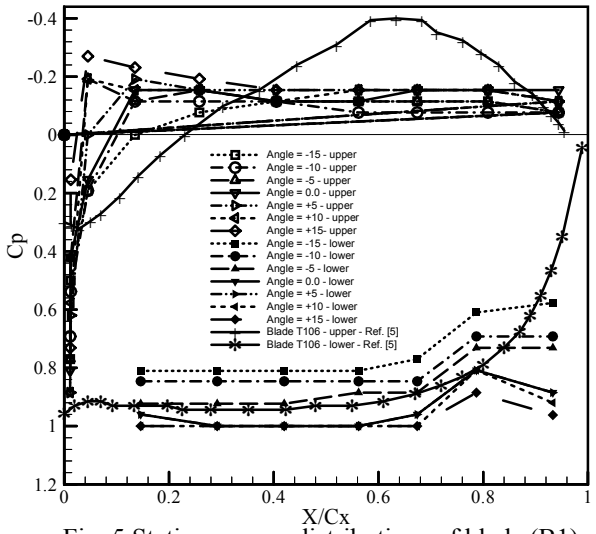

Fig. 5 Static pressure distributions of blade (B1) at Re = 166,000 for different incidence angles.

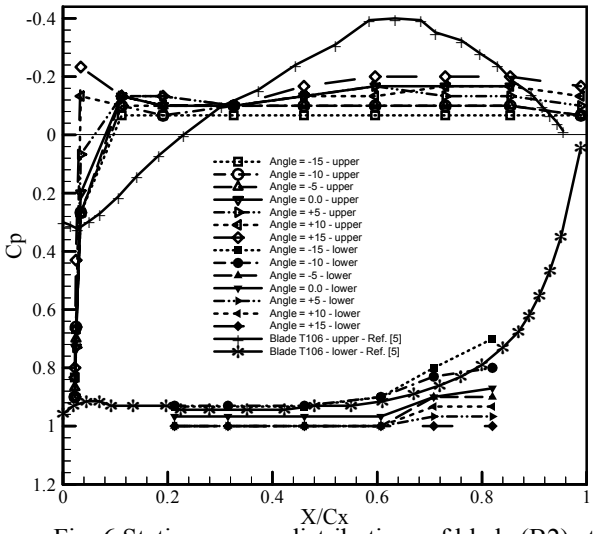

Fig. 6 Static pressure distributions of blade (B2) at Re = 166,000 for different incidence angles.

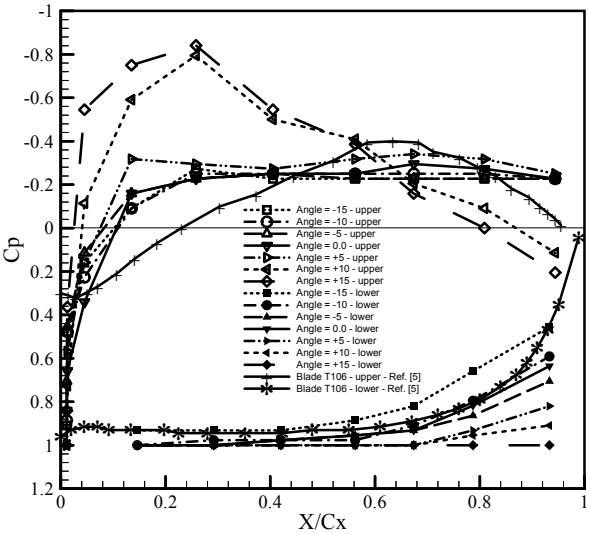

Fig. 7 Static pressure distributions of blade (B1) at Re = 202,000 for different incidence angles.

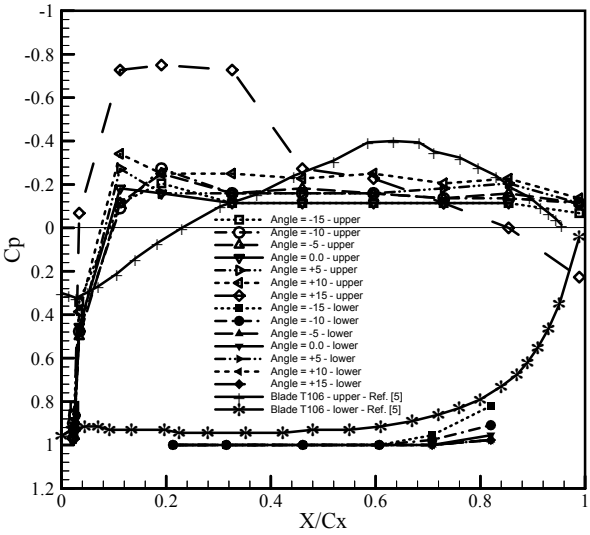

Fig. 8 Static pressure distributions of blade (B2) at Re = 202,000 for different incidence angles.

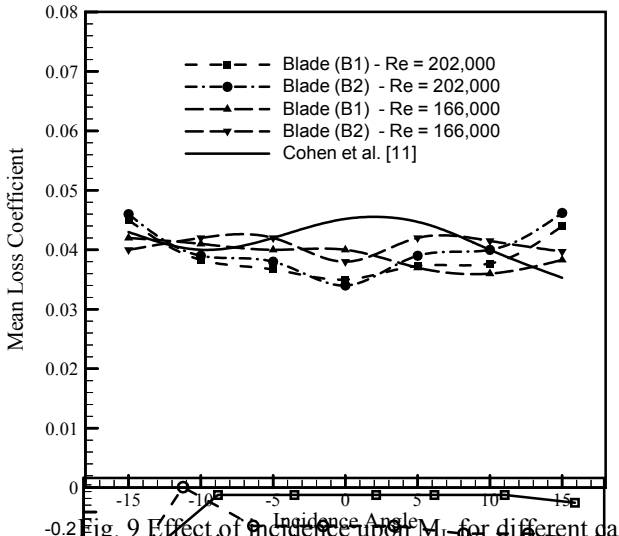

Fig. 9 Effect of incidence upon M_{1-6} for different cases.

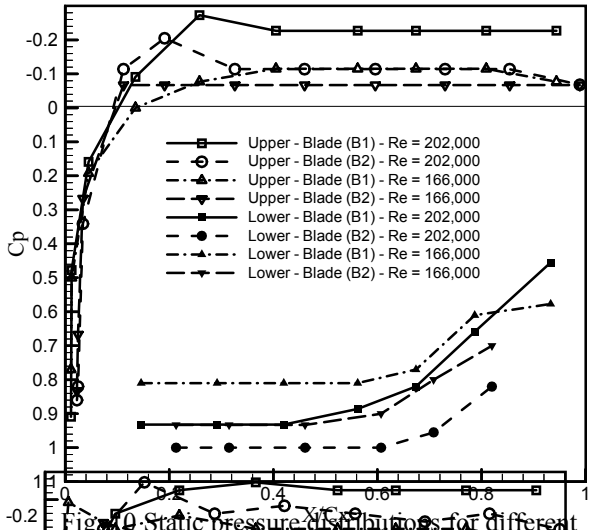

Fig. 10 Static pressure distributions for different cases at an incidence angle = -15°.

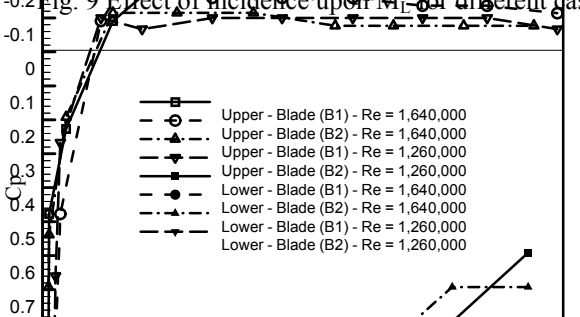

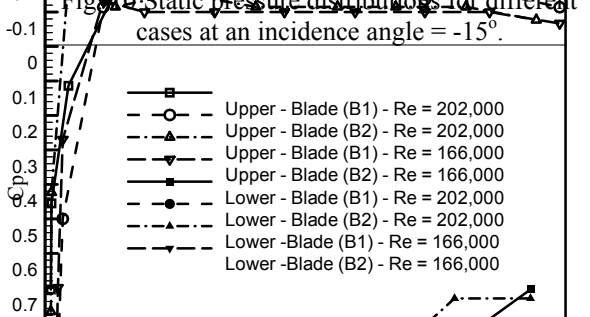

Fig. 11 Static pressure distributions for different cases at an incidence angle = -10°.

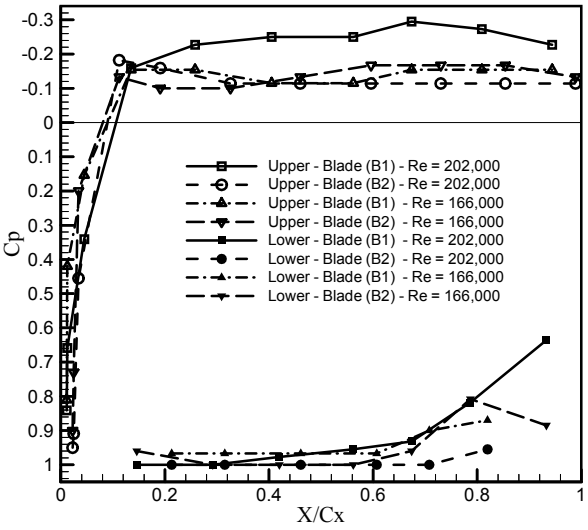

Fig. 12 Static pressure distributions for different cases at an incidence angle = -5°.

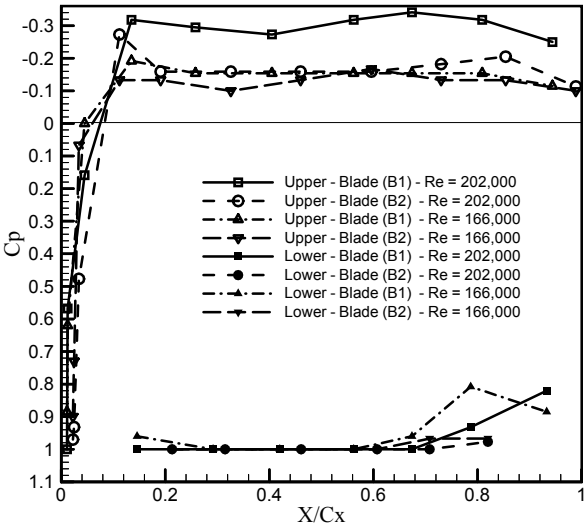

Fig. 13 Static pressure distributions for different cases at an incidence angle = 0°.

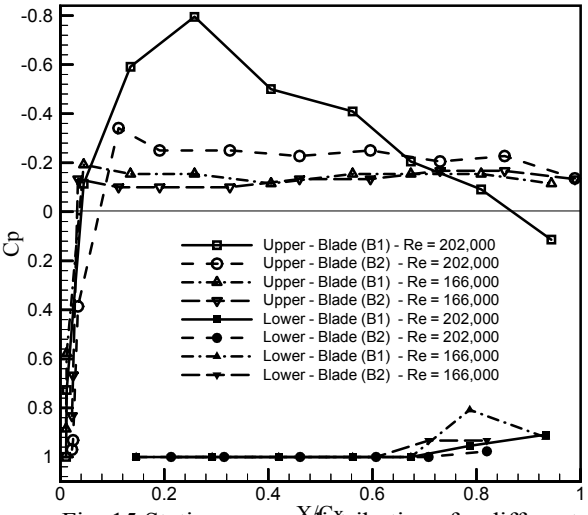

Fig. 14 Static pressure distributions for different cases at an incidence angle = +5°.

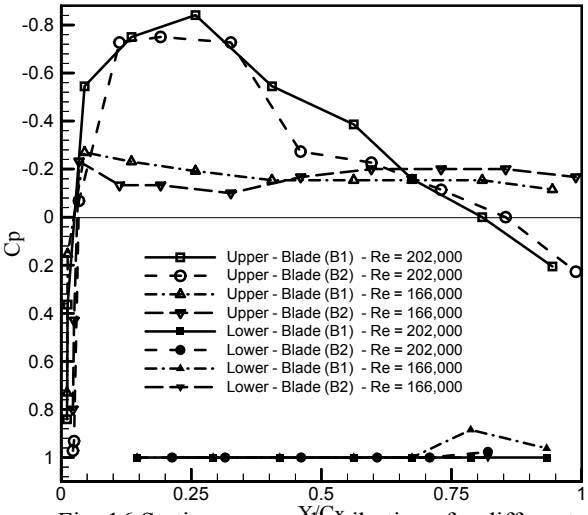

Fig. 15 Static pressure distributions for different cases at an incidence angle = +10°.

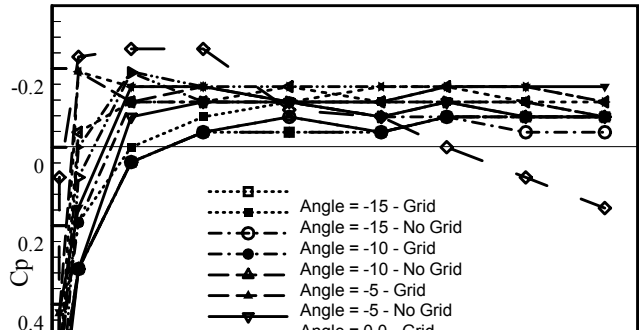

Fig. 16 Static pressure distributions for different cases at an incidence angle = +15°.

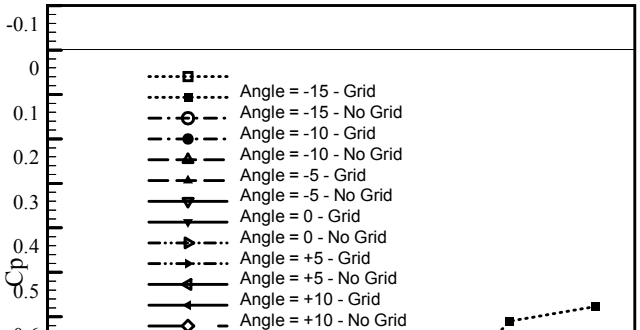

(a) Upper surface (b) Lower surface

Fig. 17 Effect of grid-generated turbulence on static pressure distribution of blade (B1) at Re = 166,000 for different incidence angles.

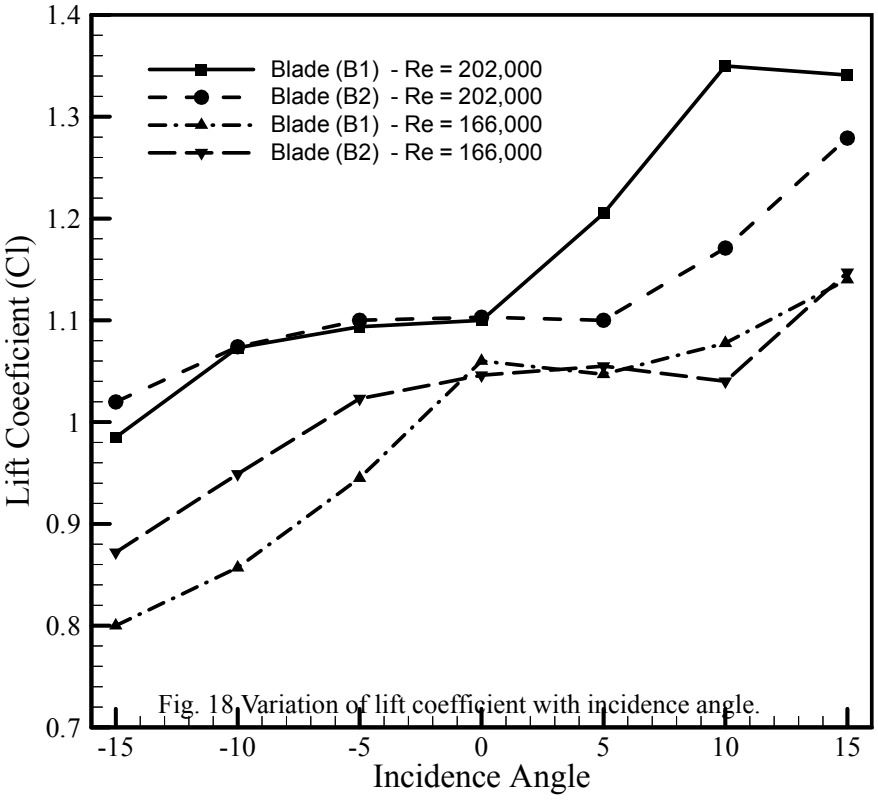

Fig. 18 Variation of lift coefficient with incidence angle.